ISSN 1807-1929
Revista Brasileira de Engenharia Agrícola e Ambiental
Brazilian Journal of Agricultural and Environmental Engineering
v.26, n.7, p.479-487, 2022
Campina Grande, PB – http://www.agriambi.com.br – http://www.scielo.br/rbeaa

DOI: http://dx.doi.org/10.1590/1807-1929/agriambi.v26n7p479-487

Relationship scales of soil arthropods and vegetation structure of Cerrado phytophysiognomies[1]

Relações de escala de artrópodes do solo e a estrutura da vegetação de fitofisionomias de Cerrado

Glécio M. Siqueira[2*] & Raimunda A. Silva[2]

[1] Research developed at Universidade Federal do Maranhão, Programa de Pós-Graduação em Biodiversidade e Biotecnologia da Amazônia, Chapadinha, Maranhão, Brazil
[2] Universidade Federal do Maranhão/Programa de Pós-Graduação em Biodiversidade e Biotecnologia da Amazônia, São Luís, Maranhão, Brazil

HIGHLIGHTS:

Soil arthropods and vegetation represent complex systems.
Soil arthropods and vegetation are related on multiple scales.
Joint correlations of soil arthropods and vegetation were stronger than their single statistical correlations.

ABSTRACT: The objective of this study was to assess the scale relationships of soil arthropods and the vegetation structure of Cerrado phytophysiognomies. The experimental plots were set in areas with dense Cerrado (T1), typical Cerrado (T2), and sparse Cerrado (T3). The edaphic fauna was collected at 128 points through pitfall traps, and the vegetation was evaluated in subplots of 9 m^2. The data were evaluated using descriptive statistics, geostatistics, multifractal analysis, and joint multifractal analysis. The soil arthropods and vegetation structure were adjusted to a geostatistical model, except for arborescent plants (T1) and arthropod abundance and arboreal plants (T2), which showed a pure nugget effect. The studied variables showed different degrees of multifractality. The graphs of joint multifractal dimension showed circular lines with high values of joint correlation for the pairs of arthropod richness versus the abundance of plant strata (r = -0.498), arthropod richness versus herbaceous plants (r = 0.323), and arthropod richness versus arboreal plants (r = 0.451) at T1. The soil fauna was influenced by the composition of the plant strata. The plots with dense Cerrado (T1) and sparse Cerrado (T3) showed the greatest spatial dependence between the samples. The multifractal analysis showed that the plot with sparse Cerrado (T3) had the greatest heterogeneity of measurement along the geometric support. In contrast, the greatest asymmetry of the singularity spectrum was described for the plot with dense Cerrado (T1). The use of geostatistical and multifractal analysis tools enabled us to characterize the scale relationships between the variables.

Key words: biological indicators, plant formations, Brazilian savanna, geostatistics, multifractal

RESUMO: O objetivo deste estudo foi avaliar as relações de escala de artrópodes do solo e da estrutura da vegetação de fitofisionomias de Cerrado. As parcelas experimentais foram alocadas em áreas com Cerrado denso (T1), Cerrado típico (T2) e Cerrado ralo (T3). A fauna edáfica foi coletada em 128 pontos, por meio de armadilhas de queda e a vegetação avaliada em subparcelas de 9 m^2. Os dados foram avaliados por meio da estatística descritiva, geoestatística, análise multifractal e joint multifractal. Os artrópodes do solo e a estrutura de vegetação se ajustaram a um modelo geoestatístico, exceto, plantas arborescentes (T1), abundância de artrópodes (T2) e plantas arbóreas (T2), que apresentaram efeito pepita puro. As variáveis estudadas apresentaram diferentes graus de multifratalidade. Os gráficos da dimensão joint multifractal mostraram linhas circulares com altos valores de correlação conjunta para riqueza de artrópodes versus abundância dos estratos vegetais (r = -0,498), riqueza de artrópodes versus herbáceos (r = 0,323) e riqueza de artrópodes versus arbóreo (r = 0,451) em T1. A fauna do solo foi influenciada pela composição dos estratos arbóreos em maior ou menor grau. As parcelas com Cerrado denso (T1) e Cerrado ralo (T3) apresentaram a maior dependência espacial entre as amostras. A análise multifractal demonstrou que a parcela com Cerrado ralo (T3) foi o sistema com maior heterogeneidade de medida ao longo do suporte geométrico; enquanto a maior assimetria do espectro de singularidade foi descrita para a parcela com Cerrado denso (T1). A utilização de ferramentas de geoestatística e análise multifractal permitiu caracterizar as relações de escala entre as variáveis.

Palavras-chave: indicadores biológicos, formações vegetais, savana brasileira, geoestatística, multifractal

• Ref. 257728 – Received 27 Oct, 2021
* Corresponding author - E-mail: gleciosiqueira@hotmail.com
• Accepted 20 Jan, 2022 • Published 04 Feb, 2022
Editors: Geovani Soares de Lima & Walter Esfrain Pereira

Introduction

The Cerrado is a heterogeneous system that presents different plant formations and comprises forest formations, savannas, and grasslands (Ribeiro & Walter, 2008). Therefore, it is necessary to understand the scales of spatial variability of soil and plant attributes in Cerrado areas using geostatistics and multifractal and joint multifractal analyses.

According to Vieira (2000), geostatistics enable the characterization of the spatial dependence between samples based on modeling and adjusting the experimental semivariogram. Gholami et al. (2017) used geostatistics to characterize the spatial distribution of tree species and soil arthropods, and Silva et al. (2018) assessed the spatial variability of soil fauna in different land use and occupation systems. Neves et al. (2010) studied the scales of spatial variability of Cerrado fragments to show that the plant strata had different scales of spatial distribution.

A multifractal analysis is applied to characterize datasets at different moments of statistical order (Banerjee et al., 2011; Biswas et al., 2012), considering different scales for a system (Halsey et al., 1986; Wilson et al., 2016; Bertol et al., 2017; Siqueira et al., 2018; Leiva et al., 2019; Silva & Siqueira, 2020). A joint multifractal analysis enables the characterization of variables on a joint scale (Banerjee et al., 2011; Biswas et al., 2012; Bertol et al., 2017; Siqueira et al., 2018; Silva et al., 2020). Thus, Siqueira et al. (2022) evaluated the scale variability between invertebrate fauna, organic carbon content, and altitude using joint multifractal analysis and concluded a positive relationship between the scales of variability in the landscape.

This study aimed to characterize the relationships between scales of soil invertebrate fauna and vegetation structures using geostatistical tools and multifractal, and joint multifractal analyses.

Material and Methods

The experimental plots are located in the municipality of Chapadinha (Maranhão, Brazil), under the geographical coordinates 3º 73' 34.68" S and 43º 32' 03.12" W, and in three vegetation types of Cerrado (Figures 1A–D). The region's climate is classified as tropical hot and humid (Aw), with the average annual temperature varying between 27 and 30 °C and average annual precipitation between 1,400 and 1,600 mm (Figure 1E). The soil of the study area is classified as Oxisol. The main physical and chemical attributes in the 0-0.2 m layer, determined according to EMBRAPA (2017), are summarized in Table 1.

Sampling was carried out on November 14, 2014, in three transects (T1, T2, and T3; Figure 1A) in an area with Cerrado vegetation. The attributes of the edaphic fauna (abundance

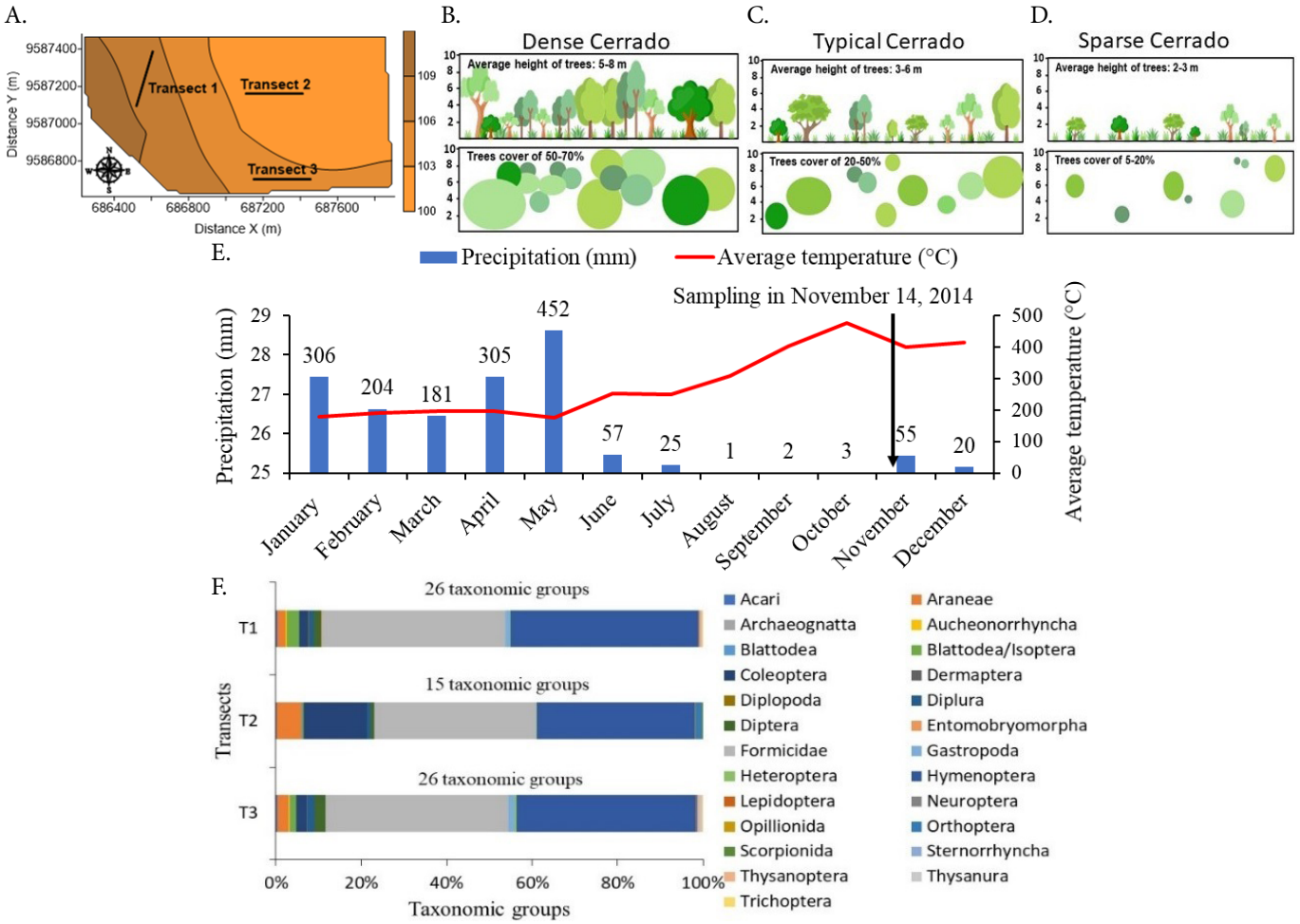

Figure 1. Topographic map and location of experimental plots (A); vegetation formations of Cerrado and tree cover profile: dense Cerrado (B), typical Cerrado (C), and sparse Cerrado (D); precipitation and air temperature in the region under study (E); abundance of the taxonomic groups of soil invertebrate fauna (F)

Table 1. Physical and chemical attributes of the surface layer of soil (0-0.2 m) in the experimental plots

	Clay	Silt	Sand	OC	pH	P	K^+	Ca^{2+}	Mg^{2+}	SB	CEC	V%
	(%)			(g dm^{-3})	($CaCl_2$)	(mg dm^{-3})	($mmol_c$ dm^{-3})					
Transect 1 (T1)	8	6	86	20	4.3	2	2.1	9	7	21.8	52.0	42.0
Transect 2 (T2)	16	6	78	12	4.3	5	3.7	6	4	19.8	48.4	40.9
Transect 3 (T3)	14	6	80	20	4.5	13	2.5	13	4	19.5	47.5	41.1

OC - Organic carbon; P - Phosphorus; K^+ - Potassium; Ca^{2+} - Calcium; Mg^{2+} - Magnesium; SB - Sum of bases; CEC - Cation exchange capacity; V% - Base saturation

and richness of arthropods) and the vegetation structure of the Cerrado [abundance of plant strata; number of herbaceous, arborescent, and arboreal plants; and average diameter at breast height (DBH 1.3 m)] were sampled over three transects containing 128 sampling points per transect, with 3 m spacing between points, totaling 381 m.

Transects were allocated to different vegetation formations of Cerrado, classified according to Ribeiro & Walter (2008): dense Cerrado (T1; Figure 1B), typical Cerrado (T2; Figure 1C), and sparse Cerrado (T3; Figure 1D). According to Aquino (2001), the edaphic fauna was sampled using pitfall traps containing 200 mL of a 4% formaldehyde solution and remained in the field for 7 days. After this period, the traps were packed in airtight containers for subsequent sorting and identification of the organisms at the order, family, and subfamily levels (Rafael et al., 2012).

In this study, 26 taxonomic groups were identified, with T1 and T3 each having all 26 and T2 having 15 taxonomic groups (Figure 1F). The abundance and richness of arthropods were determined for each sampling point from the taxonomic groups.

The vegetation structure was evaluated in subplots of 9 m^2, with the soil invertebrate fauna sampling point as the centroid. The number of plants of different heights was determined: <0.5 m (herbaceous stratum), between 0.5 and 1.3 m (arborescent stratum), and >1.3 m (tree stratum), where the average DBH (in meters; tree stratum) was also determined, according to Neves et al. (2010).

The mean, standard deviation, coefficient of variation (CV, %), asymmetry, and kurtosis were determined for the attributes under study. The normality of the data was assessed using the Kolmogorov-Smirnov test ($p \leq 0.01$). The Tukey test was used to compare the means of the variables in the experimental plots ($p \leq 0.01$).

The spatial analysis of the variables was performed using geostatistics (Vieira et al., 1997; Vieira, 2000), multifractal analysis (Hentschel & Procaccia, 1983; Halsey et al., 1986; Vidal-Vázquez et al., 2013; Siqueira et al., 2018; Silva & Siqueira, 2020), and joint and multifractal analysis (Zeleke & Si, 2006; Biswas et al., 2012; Siqueira et al., 2018).

The spatial variability of data along transects was characterized using geostatistical tools, as described by Vieira (2000). Semivariograms were computed considering the stationarity of the intrinsic hypothesis (Vieira, 2000) according to the following equation:

$$\gamma(h) = \frac{1}{2N(h)} \sum_{i=1}^{N(h)} \left[z(x_i) - z(x_i + h) \right]^2 \quad (1)$$

where:

$\gamma(h)$ - semivariogram estimated for distance h;

x - position of the measure;

h - distance between measurements; and,

N(h) - number of observations separated by distance h.

The semivariograms were adjusted to mathematical models, considering the nugget effect (C_0), structural variance (C_1), and range (a), following the procedures described by Vieira (2000).

The experimental semivariogram was adjusted by cross-validation using the methods of ordinary and weighted least squares, where the best fit was chosen according to the "jack-knifing" technique. The data presented semivariograms with a trend that was removed by the logarithmic transformation of the data.

The spatial dependency ratio (SDR, %) for the variables was calculated, considering $[C_0/(C_0 + C_1)] \times 100$, according to Cambardella et al. (1994), in which the spatial dependence was classified as strong (≤25%), moderate (between 25% and 75%), and weak (≥75%). Subsequently, scaled semivariograms were constructed for the variables that showed spatial dependence in each of the experimental plots, according to Vieira et al. (1997) Eq. 2:

$$\gamma(h)_{sc} = \frac{\gamma(h)}{Var_{(z)}} \quad (2)$$

where:

$\gamma(h)_{sc}$ - scaled semivariograms;

$\gamma(h)$ - original semivariograms; and,

$Var_{(z)}$ - data variance.

The multifractal character of the data was determined by the method of the moment, generating the partition function (Halsey et al., 1986) and the generalized dimension (Dq - Hentschel & Procaccia, 1983). The spectrum of singularity of function of f(α) versus α was generated by the direct method. The data were evaluated at intervals of 2.0, and the successive divisions for the segment (2^k), with an interval from k = 0 to k = 7, for the moments of order q (-10 < q <10) in scales of 0.5, with adjustment of coefficient of determination (R^2) > 0.90.

The total length of each transect was divided into segments (Eq. 3) and converted into a function of normalized mass $p_i(\delta)$ or $\mu_i(\delta)$, which describes the contribution of a segment or subintervals of size δ to the total mass (Eq. 4), as follows:

$$\chi(q,\delta) = \sum_{i=1}^{n(\delta)} \left[p_i(\delta) \right]^q \quad (3)$$

$$p_i(\delta) = \frac{\varphi_i(\delta)}{\sum_{i=1}^{n(\delta)} \varphi_i(\delta)} \quad (4)$$

where:

n(δ) - number of segments with size δ, whose statistical moments q are defined for $-\infty < q < +\infty$;

φi - measurement value in the i^{th} segment in scale δ; and,

$\Sigma_1^{n(\delta)}$ φi(δ) - represents the total mass of a transect.

The generalized dimension was obtained for the moments q = 0, q = 1, and q = 2 (Eqs. 5 and 6), observing when q ≠ 1 and q = 1, which makes D_1 indeterminate when it is necessary to use the rule of l' Hôpital, which was not the case in this study.

$$D_q = \frac{1}{q-1}\lim_{\delta\to 0}\frac{\log\left[\chi(q,\delta)\right]}{\log\delta} = \frac{\tau(q)}{q-1},\ \text{for } q \neq 1 \qquad (5)$$

$$D_1 = \lim_{\delta\to 0}\frac{\sum_{i=1}^{n(\delta)}\mu_i(\delta)\log\left[\chi(q,\delta)\right]}{\log\delta} = \frac{\tau(q)}{q-1},\ \text{for } q \neq 1 \qquad (6)$$

The singularity spectra were obtained through the function of f(α) versus α, which generates a parable for multifractal variables and a linear function for monofractal data (Eqs. 7 and 8).

$$\alpha(q) \propto \frac{\sum_{i=1}^{n(\delta)}\mu_i(q,\delta)\log\left[\mu_i(\delta)\right]}{\log(\delta)} \qquad (7)$$

$$f(\alpha(q)) = \propto \frac{\sum_{i=1}^{n(\delta)}\mu_i(q,\delta)\log\left[\mu_i(q,\delta)\right]}{\log(\delta)} \qquad (8)$$

The degree of multifractality (Δ – Eq. 9) and the asymmetry of the singularity spectrum (Δ – Eq. 10) were determined following the procedures described by Halsey et al. (1986):

$$\Delta = D_{-\infty} - D_{\infty} \qquad (9)$$

$$A = \frac{\alpha_0 - \alpha_{min}}{\alpha_{max} - \alpha_0} \qquad (10)$$

To assess the association of values by the joint multifractal analysis, the transect was divided into segments of size δ. The partitions were determined on the scales of measures of p (total segment of variable p) and r (total segment of variable r), which were partitioned into δ and defined as $p_i(\delta)$ and $r_i(\delta)$ (Banerjee et al., 2011; Biswas et al., 2012) (Eq. 11).

$$\mu_i(q,t,\delta) = \frac{\left[p_i(\delta)\right]^q\left[r_i(\delta)\right]^t}{\sum_{i=1}^{n(\varepsilon)}\left[p_i(\delta)\right]^q\left[r_i(\delta)\right]^t} \qquad (11)$$

where:

q and t - real numbers that represent the orders of the moment; and,

δ - scale.

The scale exponents of the function of f(α, β) determine the singularity indices α(q, t) and β(q, t) in relation to the μ_i measure (Zeleke & Si, 2006; Biswas et al., 2012; Vidal-Vázquez et al., 2013; Bertol et al., 2017; Siqueira et al., 2022) as follows:

$$\alpha(q,t) = \lim_{\varepsilon\to 0}\frac{\sum_{i=1}^{n(\varepsilon)}\left[\mu_i(q,t,\delta)\log p_i(\delta)\right]}{\log\delta} \qquad (12)$$

$$\beta(q,t) = \lim_{\varepsilon\to 0}\frac{\sum_{i=1}^{n(\varepsilon)}\left[\mu_i(q,t,\delta)\log r_i(\delta)\right]}{\log\delta} \qquad (13)$$

$$f(\alpha,\beta) = \lim_{\varepsilon\to 0}\frac{\sum_{i=1}^{n(\varepsilon)}\left[\mu_i(q,t,\varepsilon)\log(q,t,\varepsilon)\right]}{\log\varepsilon} \qquad (14)$$

The indices of the joint multifractal scale [α(q, t) and β(q, t)] were subjected to Pearson's linear correlation to determine the association on the joint scale under ($p \leq 0.01$ and $p \leq 0.05$, respectively). In addition, the relationship between pairs of variables was assessed using Pearson's linear correlation, which enabled us to evaluate the single association between variables.

Results and Discussion

In this study, 7,428 arthropods were collected [3,456 in T1, 1,629 in T2, and 2,343 in T3 (Table 2)], with T1 having the highest number of individuals (Tukey, $p < 0.01$). Regarding the average richness of arthropods, the Tukey test demonstrated statistical differences among all treatments. Vegetation composition influenced the average arthropod richness (Table 2). There was a decrease in the average arthropod richness with a decrease in tree cover (T3 < T2 < T1), confirming the results of Korboulewsky et al. (2016), Gholami et al. (2017), and Silva et al. (2018).

Thus, the composition of vegetation cover affects the invertebrate fauna of soil through its effects on the availability of food resources (Marichal et al., 2014), by improving the physical and chemical soil attributes (Korboulewsky et al., 2016) and favoring the development of suitable microclimates for soil invertebrate fauna (Silva et al., 2018).

There was no statistical difference in plant abundance between T1 and T2, whereas T3 showed a lower abundance. According to the Warrick & Nielsen (1980) classification, arthropod richness and plant attributes showed a mean CV (%), and arthropod abundance showed high CV for all 3 transects (Table 2). Thus, the differentiation among the transects describes the heterogeneity, complexity, and structure of Cerrado formations, according to Ribeiro & Walter (2008).

The spatial variability of most of the variables under study fitted to the spherical model (Table 3), whereas the abundance of arthropods and tree plants in T1 and DBH (1.3 m) in T2 fitted to a Gaussian model. The variables arborescent (T1) and abundance of arthropods and arboreal plants (T2) showed a pure nugget effect. The range values (a, m) demonstrated that

Table 2. Descriptive statistics of soil fauna and phytosociological variables in Cerrado areas

	Sum	Mean	SD	CV (%)	Skewness	Kurtosis	D*
T1 – Dense Cerrado							
Arthropod abundance	3.456	27.000 a	22.722	84.155	1.439	2.084	0.137n
Arthropod richness		5.781 a	2.416	41.806	0.475	0.999	0.167Ln
Abundance of plant strata	4.479	34.992 a	18.205	52.025	1.276	2.770	0.121n
Herbaceous	1.346	10.516 a	6.926	65.863	1.311	2.154	0.154Ln
Arborescent	1.142	8.922 a	10.071	112.881	7.671	74.435	0.216Ln
Arboreal	1.991	15.555 a	9.948	63.953	1.031	1.437	0.123n
DBH	408.950	3.220 a	2.219	68.914	2.393	7.332	0.226Ln
T2 – Typical Cerrado							
Arthropod abundance	1.629	12.727 b	10.838	85.160	1.610	3.367	0.165Ln
Arthropod richness		4.726 b	2.589	54.781	0.409	0.630	0.122n
Abundance of plant strata	4.205	32.852 a	10.764	32.765	0.527	-0.147	0.104n
Herbaceous	1.200	9.375 a	4.631	49.400	0.657	0.022	0.101n
Arborescent	1.240	9.688 a	4.543	46.899	1.090	1.858	0.144Ln
Arboreal	1.765	13.789 a	8.438	61.197	0.845	-0.004	0.123n
DBH	467	3.652 a	1.577	43.178	2.572	13.615	0.140n
T3 – Sparse Cerrado							
Arthropod abundance	2.343	18.305 b	18.837	102.910	1.384	2.303	0.166Ln
Arthropod richness		2.867 c	1.949	67.999	0.526	0.436	0.145Ln
Abundance of plant strata	3.228	25.219 b	8.800	34.893	0.474	0.952	0.094n
Herbaceous	1.254	9.797 a	5.095	52.006	0.902	1.151	0.114n
Arborescent	930	7.266 a	3.959	54.495	1.372	3.948	0.120n
Arboreal	1.044	8.156 b	3.881	47.583	0.543	0.311	0.086n
DBH	402	3.142 a	1.538	48.962	1.483	2.939	0.177Ln

DBH - Average diameter at breast height of tree plants (> 1.3 m); SD - Standard deviation; CV% - Coefficient of variation; *D - Kolmogorov–Smirnov normality test at $p \leq 0.01$; n - Normal distribution; Ln - Lognormal distribution; Mean values followed by the same letters in the column did not differ by the Tukey test ($p \leq 0.01$)

the variables had greater spatial dependence in T1 and T3, while T2 variables had lower range values. Vieira (2000) and Silva et al. (2018) stated that the pure nugget effect describes the spatial variability occurring at distances smaller than the spacing used, or homogeneity of measurements, according to Neves et al. (2010).

Studying the vegetation cover of Cerrado fragments using geostatistical tools, Neves et al. (2010) showed that the tree strata (DBH > 1.3 m), described using the range values, presented greater spatial continuity than the herbaceous strata (plants < 0.5 m), thus concluding the existence of different ranges of variability for the vegetation cover. The soil invertebrate fauna assumed similar behavior in the landscape, and the highest range values (Table 3) were described for the dense Cerrado (T1), followed by the sparse Cerrado (T3) and typical Cerrado (T2).

According to Gholami et al. (2017), the spatial structure of soil fauna occurs in scales of variability, which reflect the gradient of vegetation cover. Thus, the spatial variability of vegetation influences the diversity of edaphic communities. The higher range values for arthropod abundance and richness in T3 compared to T2 are expected, considering that 26 taxonomic groups were identified in T3 and only 15 in T2.

In this study, the spherical model adjusted the analyzed variables the most. The Gaussian model was fitted to three variables, and another three variables showed a pure nugget effect. The presence of a pure nugget effect indicates that arborescent plants in T1 and arthropod abundance and arboreal in T2 had scales of variability less than the spacing used in this study. According to Vieira (2000), there is a high spatial variability.

According to Cambardella et al. (1994), most of the variables studied showed moderate SDR values (25–75%). Nevertheless, the abundance of arthropods (SDR = 77.27%),

Table 3. Geostatistical parameters of soil fauna and phytosociological variables in Cerrado areas

Variables	Model	C_0	C_1	A (m)	SDR (%)
T1 – Dense Cerrado					
Log Arthropod abundance	Gaussian	1.70	0.50	100	77.27
Log Arthropod richness	Spherical	0.20	0.08	70	74.07
Log Abundance of plant strata	Spherical	0.30	0.25	80	54.54
Log Herbaceous	Spherical	0.60	0.53	115	53.09
Log Arborescent	Pure nugget effect				
Log Arboreal	Gaussian	1.09	0.70	110	60.89
Log DBH	Spherical	0.50	0.20	110	71.42
T2 – Typical Cerrado					
Log Arthropod abundance	Pure nugget effect				
Log Arthropod richness	Spherical	0.30	0.10	83	75.00
Log Abundance of plant strata	Spherical	0.18	0.08	65	69.23
Log Herbaceous	Spherical	0.42	0.21	70	66.66
Log Arborescent	Spherical	0.40	0.12	70	76.92
Log Arboreal	Pure nugget effect				
Log DBH	Gaussian	0.21	0.16	80	56.75
T3 – Sparse Cerrado					
Log Arthropod abundance	Spherical	1.70	0.90	110	65.38
Log Arthropod richness	Spherical	0.25	0.16	80	60.97
Log Abundance of plant strata	Spherical	0.23	0.16	60	57.50
Log Herbaceous	Spherical	0.45	0.17	80	72.58
Log Arborescent	Spherical	0.50	0.20	70	71.42
Log Arboreal	Spherical	0.40	0.27	60	59.70
Log DBH	Spherical	0.30	0.17	80	63.82

DBH - Average diameter at breast height of tree plants (> 1.3 m); C_0 - Nugget effect; C_1 - Structural variance; a - Range (m); SDR (%) - Sspatial dependency ratio

arthropod richness (SDR = 74.07%), and DBH 1.3 m (SDR = 71.42%) in T1; arthropod richness (SDR = 75.00%) and arborescent plants (SDR = 76.92%) in T2; and herbaceous plants (SDR = 72.58%) and plants between arborescent (SDR = 71.42%) in T3 showed low spatial dependence.

The scaled semivariogram (Figures 2A, C, and E) fitted values in the range of 60 m (T3) and 90 m (T1). The variables in T1 and T3 showed moderate spatial dependence (SDR =

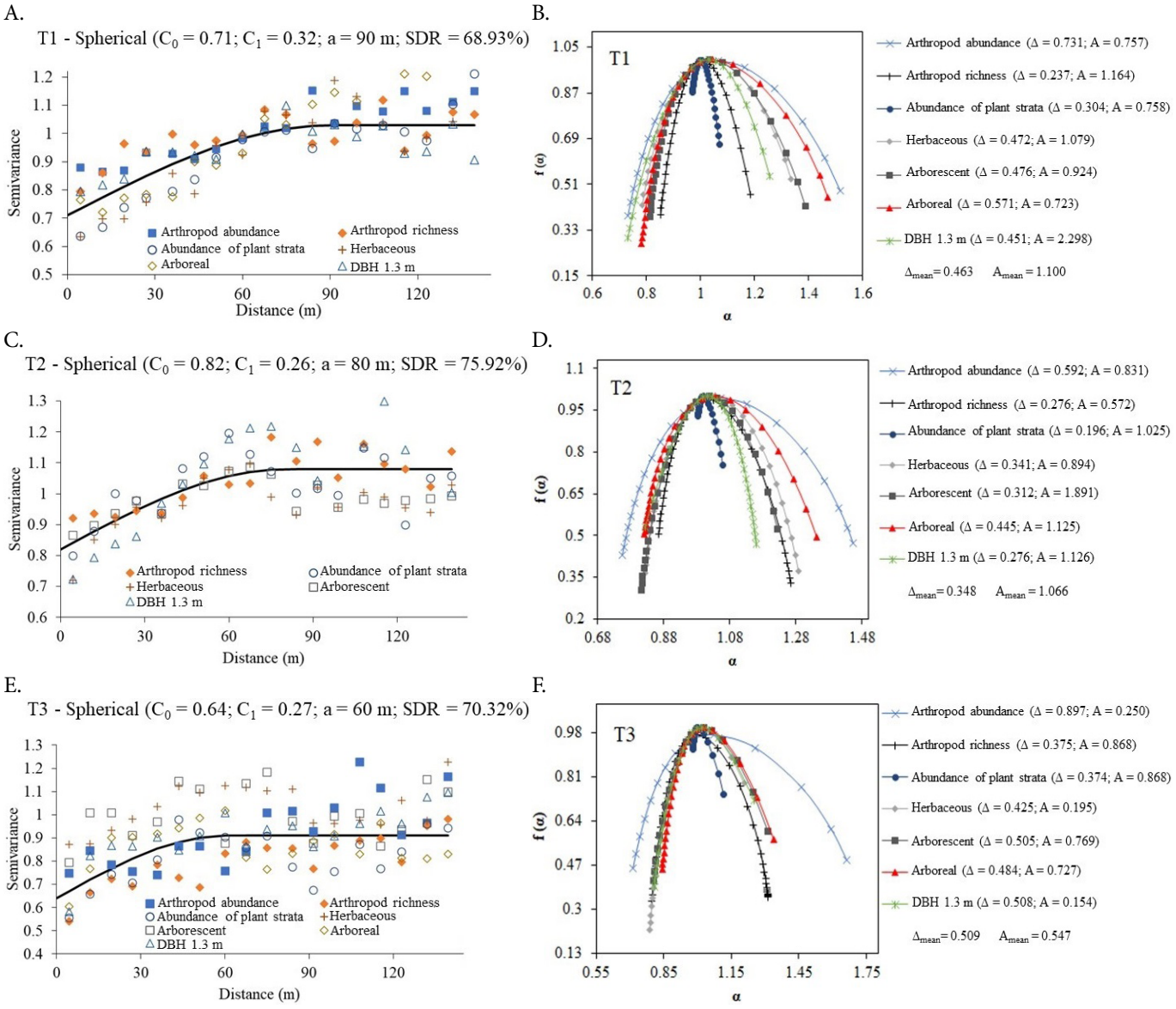

*Δ - Multifractality; A - Asymmetry

Figure 2. Scaled semivariogram and singularity spectra of soil arthropod fauna and phytosociological variables in the Cerrado areas. Scaled semivariogram (A) and singularity spectrum in T1 (B); scaled semivariogram (C) and singularity spectrum in T2 (D); and scaled semivariogram (E) and singularity spectrum in T3 (F)

25-75%), whereas T2 presented a low spatial dependence (SDR = 75.92%). The scaled semivariogram (Figures 2A, C, and E) demonstrated different scales of variability between the plots, where the adjusted scaled semivariogram in T1 had the highest range (a = 90 m), followed by T2 (a = 80 m) and T3 (a = 60 m).

According to Vieira et al. (1997), the scaled semivariogram allows grouping and comparing different variables on the same scale. All three transects showed moderate spatial dependence between samples. However, it is worth highlighting that although T3 had smaller ranges than T2, there was greater spatial dependence between the samples for the simple semivariogram, as shown by the mean values of SDR (64.48%, Table 3), and for the scaled semivariogram (SDR_{mean} = 70.32%; Figures 2A, C, and E).

All variables showed multifractal behavior, which was assessed using the singularity spectrum (Figures 2B, D, and F), with different degrees of multifractality (Δ) and asymmetry (A). The multifractal spectrum constructed for the Dq moment interval (q = 10 and q = -10) showed different degrees of multifractality (Δ) and asymmetry (A), reflecting moderate heterogeneity (Figures 2B, D, and F).

The highest and lowest degree of multifractality in T1 was described for arthropod abundance (Δ = 0.731; Figure 2B) and arthropod richness (Δ = 0.237). In T2, the lowest value corresponded to the abundance of plant strata (Δ = 0.196) and the highest to arthropod abundance (Δ = 0.592; Figure 2D). In T3, the lowest value was described for the abundance of plant strata (Δ = 0.374) and the highest for arthropod abundance (Δ = 0.897; Figure 2F).

The lowest asymmetry value for singularity spectra was described for DBH (1.3 m) in T3 (Δ = 0.154), whereas the highest was reported for DBH (1.3 m) in T1 (A = 2.298). In general, T3 and T2 showed the lowest asymmetry for the pairs of variables (Δ = 0.525 and Δ = 1.066, respectively), while T1 presented the highest average asymmetry (Δ = 1.100).

The abundance of arthropods in all 3 transects showed different degrees of multifractality (Δ). T3 was the most heterogeneous (Δ = 0.897). In contrast, T2 showed the lowest

degree of multifractality for the abundance of arthropods (Δ = 0.592, Figure 2D), indicating that this variable was more homogeneous along the transect.

T1 and T3 had the lowest values of average multifractality (Δ = 0.463 and Δ = 0.348, respectively) for the variables under study, as they were more homogeneous environments than T2. However, each of them had particularities, the tree layer was predominant in T1, and the herbaceous layer dominated in T3. Therefore, the multifractal scales of the singularity spectrum reflected the heterogeneity or homogeneity of the different vegetation formations, as reported by Vidal-Vázquez et al. (2013) and Silva & Siqueira (2020).

In general, the singularity spectra described asymmetry (Figures 2B, D, and F) for the branches on the left, indicating the dominance of high measurement values along the transect. According to Bertol et al. (2017) and Siqueira et al. (2018), the asymmetry of the branches of the singularity spectrum to the right or left provides important information on the degree of heterogeneity and domains of measurement of the scales of a system.

The singularity spectra for the abundance of plant strata showed similar behavior for the three plots studied; however, it appears that there was a variability in the scales associated with low measurement values distributed along the geometric support. Regarding arthropod richness, T2 and T3 showed singularity spectra elongated to the right, describing the domain of low measurement values distributed over the transects (Zeleke & Si, 2006; Vidal-Vázquez et al., 2013; Yakimov et al., 2014; Wilson et al., 2016; Leiva et al., 2019; Siqueira et al., 2022).

The graphs of the joint multifractal distribution were obtained using the function of f(α, β) and are shown in Figure 3.

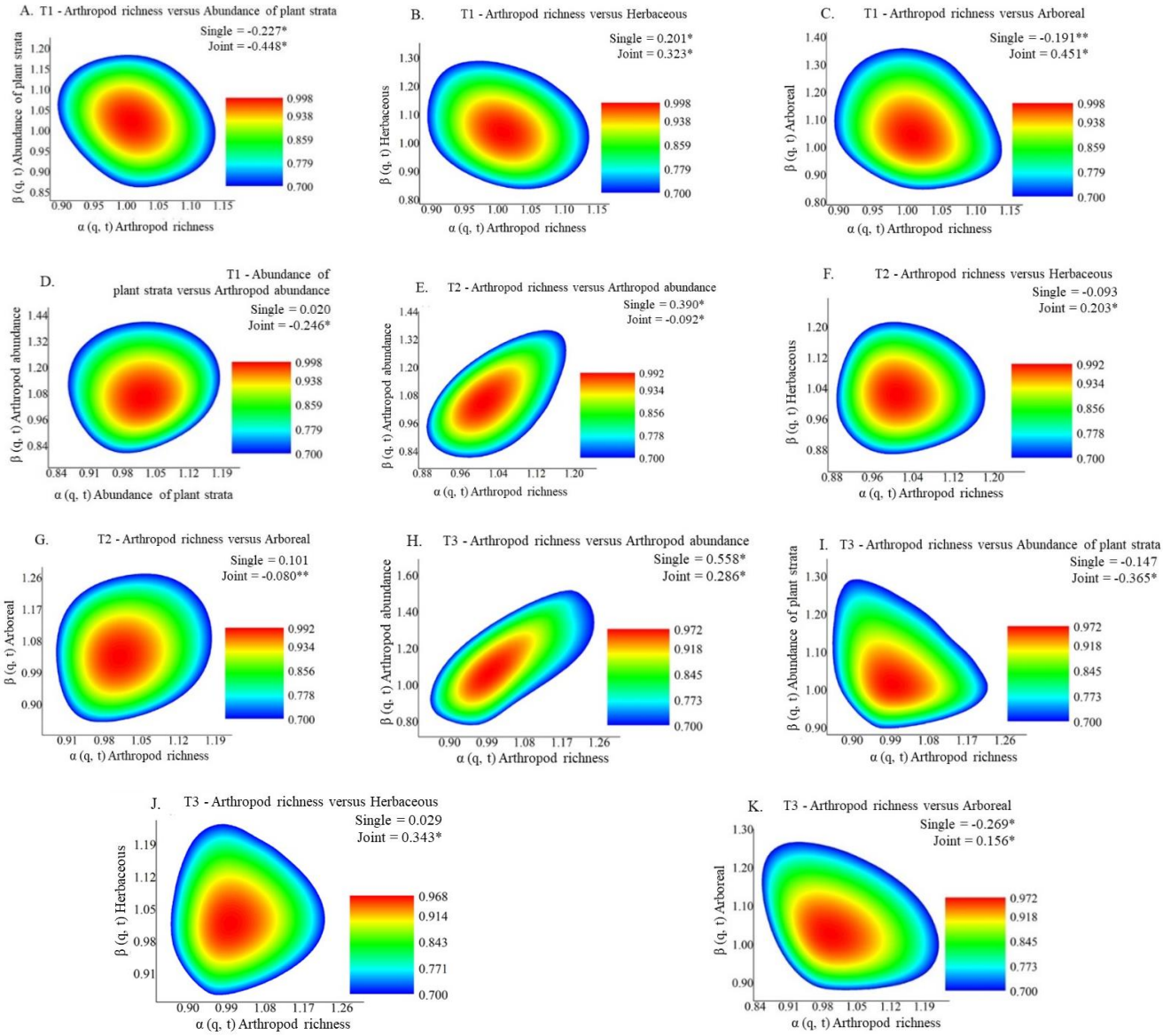

The different colors indicate the joint dimensions of the two scale indices. * $p \leq 0.01$ and ** $p \leq 0.05$ by t-test

Figure 3. Joint multifractal distribution for soil fauna and vegetation attributes: T1, arthropod richness versus the abundance of plant strata (A); arthropod richness versus herbaceous (B); arthropod richness versus arboreal (C); abundance of plant strata versus arthropod abundance (D); T2, arthropod richness versus abundance (E); arthropod richness versus herbaceous (F); arthropod richness versus arboreal (G); T3, arthropod richness versus abundance (H); arthropod richness versus the abundance of plant strata (I); arthropod richness versus herbaceous (J); and arthropod richness versus arboreal (K). Pearson's correlation at $p \leq 0.01$ and $p \leq 0.05$ on a simple and joint multifractal scale

Only the graphs showing Pearson's correlation on a multifractal joint scale are displayed.

The graphs of the joint multifractal spectrum [f (α, β); Figure 3] are represented by contour lines that express the scale relationship of the distribution of values between two variables (Zeleke & Si, 2006; Banerjee et al., 2011; Biswas et al., 2012; Siqueira et al., 2022). The association with high values is represented in the lower-left part, whereas the upper-right part is the association with low values (Zeleke & Si, 2006).

According to Biswas et al. (2012), the circular graphics of the joint multifractal spectrum [f(α, β); Figure 3] indicate that there is no association on the scales of variable distribution, while graphics with an elliptical form show an association with positive or negative values on the scales of variable distribution.

The graph of the joint multifractal distribution for arthropod richness versus abundance in T2 ($r = -0.092$, $p \leq 0.05$; Figure 3E) and T3 ($r = 0.286$, $p \leq 0.01$; Figure 3H) presented elliptical contour lines. This indicates an association in the joint distribution scales with high and low values of f(α, β) (Banerjee et al., 2011; Biswas et al., 2012; Siqueira et al., 2018; Silva et al., 2020; Siqueira et al., 2022). The other graphs shown in Figure 3 have contour lines with a circular distribution, demonstrating that there are no joint multifractal associations on the distribution scales for the represented variables.

Geostatistical tools and multifractal and joint multifractal analyses showed that soil invertebrate fauna attributes and vegetation composition presented different scales of variability. The geostatistical analysis described that the variables have similar scales of variability when considering the particularities of each phytophysiognomy of the Cerrado. T2 (typical Cerrado) presented the lowest spatial continuity among the samples, describing a certain data heterogeneity. According to Ribeiro & Walter (2008), the typical Cerrado is an intermediate environment to the dense Cerrado and sparse Cerrado, thus justifying the lower spatial continuity between the samples.

The more homogeneous environments, T1 with predominantly tree species and T3 with predominantly herbaceous species, showed the greatest spatial continuity in the samples. The multifractal analysis was important for describing the scales of spatial variability along the geometric support, characterizing systems with greater or lesser multifractality and indicating the presence of high or low measurement values along the transects.

Multifractal analysis proved an important tool for describing scale variability. In addition, the joint multifractal analysis described the magnitude of the relationships of the joint scales [f(α, β)], enabling us to ascertain whether the measurement values of the pairs of variables have a spatial association in the geometric support. This is an important tool for environmental studies, as it enables investigating the variables with the potential for predicting other variables, as described by Siqueira et al. (2018).

Conclusions

1. The soil arthropods and vegetation structure of Cerrado phytophysiognomies showed relationships on multiple scales.

2. The dense Cerrado (T1) and sparse Cerrado (T3) showed the greatest spatial dependence among the samples.

3. Based on the multifractal analysis, the sparse Cerrado (T3) had the greatest heterogeneity of measurement along the geometric support. In contrast, the greatest asymmetry of the singularity spectrum was described for the dense Cerrado (T1).

4. The use of geostatistics and multifractal analysis enabled us to characterize the scale relationships between the variables.

Acknowledgments

The authors would like to thank the Fundação de Amparo à Pesquisa e ao Desenvolvimento Científico e Tecnológico do Maranhão (FAPEMA – process BD-02105/17, COOP-04938/18, BEST-EXT-00361/19, BINST-00362/19, UNIVERSAL-00976/19 and POS-GRAD-02423/21), and the Conselho Nacional de Desenvolvimento Científico e Tecnológico (CNPq - Process 312515/2020-0). This study was financed in part by the Coordenação de Aperfeiçoamento de Pessoal de Nível Superior (CAPES- Finance Code 001).

Literature Cited

Aquino, A. M. Manual para coleta da macrofauna do solo. Seropédica: Embrapa, 2001. 20p

Banerjee, S.; He, Y.; Guo, X.; Si, B. C. Spatial relationships between leaf area index and topographic factors in a semi-arid grassland joint multifractal analysis. Australian Journal of Crop Science, v.6, p.756-763, 2011

Bertol, I.; Schick, J.; Bandeira, D. H.; Paz-Ferreiro, J.; Vázquez, E. V. Multifractal and joint multifractal analysis of water and soil losses from erosion plots: A case study under subtropical conditions in Santa Catarina highlands, Brazil. Geoderma, v.287, p.116-125, 2017. https://doi.org/10.1016/j.geoderma.2016.08.008

Biswas, A.; Cresswell, H. P.; Si, B. C. Application of multifractal and joint multifractal analysis in examining soil spatial variation: A review. Fractal Analysis and Chaos in Geosciences, v.6, p.109-138, 2012. https://doi.org/10.5772/51437

Cambardella, C. A.; Moorman, T. B.; Novak, J. M.; Parkin, T. B.; Karlen, D. L.; Turco, R. F.; Konopka, A. E. field scale variability of soil properties in central Iowa soil. Soil Science Society of America Journal, v.58, p.1501-1511, 1994. https://doi.org/10.2136/sssaj1994.03615995005800050033x

EMBRAPA - Empresa Brasileira de Pesquisa Agropecuária. Manual de métodos de análise de solo. Brasília: Embrapa, 2017. 574p.

Gholami, S.; Sheikhmohamadi, B.; Sayad, E. Spatial relationship between soil macrofauna biodiversity and trees in Zagros forests, Iran. Catena, v.159, p.1-8, 2017. http://dx.doi.org/10.1016/j.catena.2017.07.021

Halsey, T. C.; Jensen, M. H.; Kadanoff, L. P.; Procaccia, I.; Shraiman, B. I. Fractal measures and their singularities: the characterization of strange sets. Physical Review - Part A, v.33, p.1141-1151, 1986. https://doi.org/10.1103/PhysRevA.33.1141

Hentschel, H. G. E.; Procaccia, I. The infinite number of generalized dimensions on fractals and strange attractors. Physica D, v.8, p.435-444, 1983. https://doi.org/10.1016/0167-2789(83)90235-X

Korboulewsky, N.; Perez, G.; Chauvat, M. How tree diversity affects soil fauna diversity: A review. Soil Biology and Biochemistry, v.94, p.94-106, 2016. https://doi.org/10.1016/j.soilbio.2015.11.024

Leiva, J. R.; Silva, R. A.; Buss, R. N.; França, V. L.; Souza, A. A.; Siqueira, G. M. Multifractal analysis of soil penetration resistance under sugarcane cultivation. Revista Brasileira de Engenharia Agrícola e Ambiental, v.23, p.538-544, 2019. https://doi.org/10.1590/1807-1929/agriambi.v23n7p538-544

Marichal, R.; Grimaldi, M.; Feijoo M., A.; Oszwald, J.; Praxedes, C.; Ruiz Cobo, D. H.; del Pilar Hurtado, M.; Desjardins, T.; Silva Junior, M. Ld; Silva Costa, L. Gd; Miranda, I. S.; Delgado Oliveira, M. N.; Brown, G. G.; Tsélouiko, S.; Martins, M. B.; Decaëns, T.; Velasquez, E.; Lavelle, P. Soil macroinvertebrate communities and ecosystem services in forested landscapes of Amazonia. Applied Soil Ecology, v.83, p.177-185, 2014. https://doi.org/10.1016/j.apsoil.2014.05.006

Neves, D. A.; Lemos, F.; González, A. P.; Vieira, S. R.; Siqueira, G. M. Using geostatistics for assessing biodiversity of forest reserve areas. Bragantia, v.69, p.131-140, 2010. https://doi.org/10.1590/S0006-87052010000500014

Rafael, J. A.; Melo, G. A. R.; Carvalho de, C. J. B.; Casari, S. A.; Constantino, R. Insetos do Brasil: Diversidade e taxonomia. Ribeirão Prêto: Holos Editora, 2012. 810p.

Ribeiro, J. F.; Walter, B. M. T. As principais fitofisionomias do bioma cerrado. In: Sano, S. M.; Almeida de, S. P.; Ribeiro, J. F. Cerrado: Ecologia e flora. Brasília: Embrapa Cerrados, 2008. 876p.

Silva, E. F. F., Garcia-Tomillo, A., Souza de, D. H. S., Vidal-Vázquez, E., Siqueira, G. M., Dantas, D. da C., Paz-Gonzalez, A. Multifractal and joint multifractal analysis of soil micronutrients extracted by two methods along a transect in a coarse-textured soil. European Journal of Soil Science, v.71, p.1-9, 2020. https://doi.org/10.1111/ejss.13052

Silva, R. A.; Siqueira, G. M. Multifractal analysis of soil fauna diversity indices. Bragantia, v.79, p.120-133, 2020. https://doi.org/10.1590/1678-4499.20190179

Silva, R. A.; Siqueira, G. M.; Costa, M. K. L.; Guedes Filho, O.; Silva, ÊFdFe Spatial variability of soil fauna under different land use and managements. Revista Brasileira de Ciência do Solo, v.42, p.1-18, 2018. https://doi.org/10.1590/18069657rbcs20170121

Siqueira, G. M.; Silva, E. F. de F.; Vidal-Vázquez, E.; Paz-González, A. Multifractal and joint multifractal analysis of general soil properties and altitude along a transect. Biosystems Engineering, v.168, p.105-120, 2018. https://dx.doi.org/10.1111/ejss.13052

Siqueira, G. M.; Souza, A. A.; Albuquerque, P. M. C.; Guedes Filho, O. Multifractal and joint multifractal analysis of soil invertebrate fauna, altitude, and organic carbon. Revista Brasileira de Engenharia Agrícola e Ambiental. v. 26, p.248-257, 2022. https://doi.org/10.1590/1807-1929/agriambi.v26n4p248-257

Vidal-Vázquez, E.; Camargo, O. A.; Vieira, S. R.; Miranda, J. G. V.; Menk, J. R. F.; Siqueira, G. M.; Mirás-Avalos, J. M.; Paz González, A. Multifractal analysis of soil properties along two perpendicular transects. Vadose Zone Journal, v.12, p.1-13, 2013. https://doi.org/10.2136/vzj2012.0188

Vieira, S. R. Geoestatística em estudos de variabilidade espacial do solo. In: SOLO Novais, R. F.; Alvarez, V. V. H.; Schaefer, C. E. G. R. Tópicos em ciência do solo. Viçosa: Sociedade Brasileira de Ciência do Solo, p.1-54, 2000.

Vieira, S. R.; Tillotson, P. M.; Biggar, J. W.; Nielsen, D. R. Scaling of semivariograms and the kriging estimation of field-measured properties. Revista Brasileira de Ciência do Solo, v.21, p.525-533, 1997. https://doi.org/10.1590/S0100-06831997000400001

Warrick, A. W.; Nielsen, D. R. Spatial variability of soil physical properties in the field. In: Hillel, D. Applications of soil physics. New York: Academic Press, p.319-344, 1980.

Wilson, M. G.; Mirás-Avalos, J. M.; Lado, M.; Paz-González, A. Multifractal analysis of vertical profiles of soil penetration resistance at varying water contents. Vadose Zone Journal, v.15, p.1-10, 2016. https://doi.org/10.2136/vzj2015.04.0063

Yakimov, B. N.; Solntsev, L. A.; Rozenberg, G. S.; Iudin, D. I.; Shirokov, A. I.; Lokteva, O. A.; Gelashvili, D. B. Local multifractal analysis of the spatial structure of Meadow communities at small scale. Doklady Biological Sciences: Proceedings of the Academy of Sciences of the USSR, Biological Sciences Sections, v. 458, p.297-301, 2014. https://doi.org/10.1134/S0012496614050123

Zeleke, T. B.; Si, B. C. Characterizing scale-dependent spatial relationships between soil properties using multifractal techniques. Geoderma, v.134, p.440-452, 2006. https://doi.org/10.1016/j.geoderma.2006.03.013